Volume 58(7): 653–668, 2010
Journal of Histochemistry & Cytochemistry
http://www.jhc.org

ARTICLE

Cellular Distribution and Subcellular Localization of mCLCA1/2 in Murine Gastrointestinal Epithelia

Eleni Roussa, Petra Wittschen, Natascha A. Wolff, Blazej Torchalski, Achim D. Gruber, and Frank Thévenod

Department of Molecular Embryology, Institute for Anatomy and Cell Biology II, University of Freiburg, Freiburg, Germany (ER); Department of Veterinary Pathology, Freie Universität Berlin, Berlin, Germany (PW,ADG); and Institute of Physiology and Pathophysiology, University of Witten/Herdecke, Witten, Germany (NAW,BT,FT)

SUMMARY mCLCA1/2 are members of the CLCA protein family that are widely expressed in secretory epithelia, but their putative physiological role still awaits elucidation. mCLCA1/2 have 95% amino acid identity, but currently no specific antibody is available. We have generated a rabbit polyclonal antibody (pAb849) against aa 424–443 of mCLCA1/2. In HEK293 cells transfected with mCLCA1; pAb849 detected two specific protein bands at ~125 kDa and 90 kDa, representing full-length precursor and N-terminal cleavage product, respectively. pAb849 also immunoprecipitated mCLCA1 and labeled the protein by immunostaining. But pAb849 crossreacted with mCLCA3/4/6 despite ≤80% amino acid identity of the antigenic epitope. We therefore investigated the cellular localization of mCLCA1/2 in epithelial tissues, which do not express mCLCA3/4/6 (salivary glands, pancreas, kidney) or express mCLCA3/6 with known localization (mucus cells of stomach and small intestine; villi of small intestine). *mCLCA1/2* mRNA and protein expression were found in both parotid and submandibular gland, and immunohistochemistry revealed labeling in parotid acinar cells, in the luminal membrane of parotid duct cells, and in the duct cells of submandibular gland. In exocrine pancreas, mCLCA1/2 expression was restricted to acinar zymogen granule membranes, as assessed by immunoblotting, immunohistochemistry, and preembedding immunoperoxidase and immunogold electron microscopy. Moreover, mCLCA1/2 immunolabeling was present in luminal membranes of gastric parietal cells and small intestinal crypt enterocytes, whereas in the kidney, mCLCA1/2 protein was localized to proximal and distal tubules. The apical membrane localization and overall distribution pattern of mCLCA1/2 favor a transmembrane protein implicated in transepithelial ion transport and protein secretion. **(J Histochem Cytochem 58:653–668, 2010)**

KEY WORDS
calcium-activated chloride channel
mCLCA1/2
mouse
pancreas
salivary glands
parietal cells
kidney
transmembrane protein
zymogen granules

SECRETORY AND REABSORBING EPITHELIA are equipped with a set of channels and transporters in their apical and basolateral membranes that enable transepithelial transport of fluid and electrolytes. Epithelial cells of the secretory endpieces of exocrine glands, such as salivary glands and pancreas, are additionally specialized to secrete proteins. The processes of secretion of ions and secretion of proteins by acinar cells are associated with elevation of cytosolic Ca^{2+} concentration ($[Ca^{2+}]_{cyt}$). An increase in $[Ca^{2+}]_{cyt}$ evoked by secretagogues causes the opening of basolaterally located K^+ and apically located Cl^- channels, and the movement of secretory granules or vesicles toward the apical membrane and their fusion with the membrane to begin the process of exocytosis (Melvin 1999; Thévenod 2002; Williams 2006).

Correspondence to: Frank Thévenod, MD, PhD, ZBAF, Institute of Physiology and Pathophysiology, University Witten/Herdecke, Stockumer Str. 12 (Thyssenhaus), D-58453 Witten, Germany. E-mail: frank.thevenod@uni-wh.de

Received for publication October 8, 2009; accepted April 1, 2010 [DOI: 10.1369/jhc.2010.955211].

The molecular identity of Ca^{2+}-activated Cl^- channels (CaCC) has been an enigmatic issue for many years. Among several alternatives, members of the CLCA family have been considered as promising candidates (Loewen and Forsyth 2005). However, in recent years, the question of whether CLCA proteins can form Cl^- channels per se, may function as mediators of other Cl^- channels, or are secreted soluble proteins has been controversially discussed (Hartzell et al. 2005; Patel et al. 2009). Among the members of the CLCA family, the hCLCA1 and its mouse ortholog, mCLCA3, have been well characterized (Gandhi et al. 1998; Agnel et al. 1999). Based on its biophysical properties and on analysis of the posttranslational processing and intracellular trafficking, experimental evidence has suggested that this protein is a secreted one and functions as a signaling molecule rather than as a channel (Gibson et al. 2005; Mundhenk et al. 2006). Along this line of thinking and together with its putative cellular distribution, it has been proposed that mCLCA3 is involved in the regulation of mucus secretion.

Analysis of the protein structure of different CLCA isoforms has revealed that members of the CLCA family share common properties, such as the presence of a proteolytic cleavage site. Thereby, a precursor ~125-kDa glycoprotein is cleaved to produce ~90-kDa and ~35-kDa cleavage products. However, members of the CLCA family may also considerably differ from each other. mCLCA1 is the only member of the CLCA family that is able to produce Ca^{2+}-activated Cl^- currents that resemble those of endogenous CaCCs when coexpressed with KCNMB1 (Greenwood et al. 2002). Previously, we have identified a CLCA protein in rat zymogen granule membranes (ZGMs) with an antiserum against bovine CLCA1 that could be part of a Ca^{2+}-activated HCO_3^- conductance of rat secretory granules (Thévenod et al. 2003).

Although the membrane protein TMEM16A, recently identified and cloned, exhibits the characteristics of a CaCC (Caputo et al. 2008; Schroeder et al. 2008; Yang et al. 2008), the physiological significance and function of each CLCA isoform still await elucidation. As a first step, tissue distribution and exact subcellular localization of mCLCA proteins in various tissues would greatly contribute to the understanding of their putative function.

The present study was therefore undertaken to attain first insights into the putative roles of mCLCA1/2, which are widely expressed in secretory epithelia and other tissues (Gruber et al. 1998b), but no specific antibody against these proteins is currently available. We have generated and characterized rabbit polyclonal antibodies against mCLCA1/2, which show 95% identity at the protein level and are therefore barely distinguishable by immunological techniques, and assessed their cellular localization in murine salivary glands, stomach, small intestine, and kidney. The results show that mCLCA1/2 are localized in pancreatic ZGMs, in submandibular granular duct cells, in the luminal membranes of parotid and submandibular ducts, in gastric parietal and small intestinal crypts, and in renal distal and proximal tubule cells. The overall distribution pattern of mCLCA1/2 argues against a nature as secreted protein and favors their contribution in transepithelial ion transport and protein secretion.

Materials and Methods

Generation of Antibodies

Peptide sequences of high predicted immunogenicity were selected from the mCLCA1 open reading frame (accession no. gi:32964827) using computer-aided antigenicity analyses. A commercial service (ImmunoGlobe; Himmelstadt, Germany) was used for antibody generation. Three oligopeptides were synthesized (pAb847, corresponding to aa 68 QGRVYFRNISILVPMT 83; pAb848, corresponding to aa 385 TSICHGLQAGFQAITS 400; and pAb849 corresponding to aa 424 CFEAVSRSGAIIHTIALGPS 443). The oligopeptides were coupled to keyhole limpet hemocyanin and used for standard immunization of two rabbits each. Preimmune sera were collected before immunization and used as controls in immunoblot experiments. Following initial testing of antiserum immunoreactivity, the pAb849 antibody was affinity-immunopurified using the corresponding peptide coupled to an EAH-sepharose column (ImmunoGlobe). The experiments in the present study were performed with affinity-purified antibodies.

FLAG-tagging of mCLCA1

The FLAG epitope was introduced near the carboxy terminus between residues of aa 757 and 758 by site-directed mutagenesis (QuikChange II Site-Directed Mutagenesis Kit; Stratagene, Amsterdam, The Netherlands), using loop-forming primers containing the FLAG sequence flanked by regions complementary to adjacent regions of *mCLCA1* (the FLAG sequence is underlined). Sense, GACCACGCTCGTGTGTTCCCA-GACTACAAGGACGACGATGACAAGCCAAG-TAAAGTCACAGACCTGG; anti-sense, CCAGGTCTGTGACTTTACTTGGCTTGT-CATCGTCGTCCTTGTAGTCTGGGAACACAC-GAGCGTGGTC.

Cycling conditions were as follows: 95C for 30 sec, 1 cycle; 95C for 30 sec, 55C for 1 min, and 68C for 8.5 min, 18 cycles.

Transient Transfection of HEK293 Cells

HEK293 cells (human embryonic kidney cortex cells, CRL-1573; American Type Culture Collection, Rockville, MD) were grown in 6-well plates using

DMEM + 1 g/liter D-glucose + GlutaMAX I + pyruvate supplemented with 10% heat-inactivated FBS (Invitrogen; Karlsruhe, Germany) at 37C in a humidified 5% CO_2 atmosphere and 120 U/ml penicillin and 120 μg/ml streptomycin (Invitrogen). HEK293 cells were transfected with either pcDNA3.1 plasmid (Invitrogen) containing the *mCLCA1-3, 5, 6* open reading frames (Leverkoehne and Gruber 2002; Leverkoehne et al. 2002; Beckley et al. 2004; Evans et al. 2004) and FLAG-tagged *mCLCA1* or pIRES2-EGFP plasmid (Clontech; Saint-Germain-en-Laye, France) containing the *mCLCA4* open reading frame (Elble et al. 2002) using Lipofectamine 2000 (Invitrogen) according to the manufacturer's protocol. *mCLCA4* and *mCLCA5* plasmids were kind gifts of Dr. R.C. Elble (Department of Pharmacology and Cancer Institute, Southern Illinois University School of Medicine, Springfield, IL). Cells transfected with pcDNA3.1 or pIRES2-EGFP vector alone served as negative controls (mock-transfected). In brief, 24 hr before transfection, 1×10^5-1×10^6 cells per well were seeded in serum-containing but antibiotic-free medium. Lipofectamine 2000 transfection cocktail was prepared by diluting 0.8 μg of plasmid DNA in 50 μl of serum-free medium without antibiotics. Lipofectamine 2000 reagent (2 μl) was also diluted into 50 μl of medium and allowed to stand for 5 min at room temperature. Lipofectamine 2000 and plasmid solutions were combined, mixed, and incubated for an additional 20 min at room temperature. Meanwhile, the medium from cells was aspirated and replaced by 0.5 ml fresh serum-containing medium without antibiotics. The Lipofectamine 2000/plasmid mixture was carefully added to cells, and the dishes were gently swirled to mix. Cells were then returned to the incubator and incubated for additional 18–48 hr. When necessary, the medium was replaced by fresh medium 1 day post-transfection.

Isolation of Zymogen Granules (ZGs) and Purification of ZGMs

Procedures were approved by the animal ethics committee, and animal handling was in accordance with German law on animal experimentation and the European Directive for the Protection of Vertebrate Animals Used for Experimental and Other Scientific Purposes (86/609/EU). ZGs from mouse exocrine pancreas were isolated as described in detail elsewhere (Thévenod et al. 2003; Lee et al. 2008). Briefly, pancreatic tissue from female C57BL/6N mice (15–17 g, fasted overnight) (Charles River Laboratories; Sulzfeld, Germany) was homogenized by nitrogen pressure cavitation and centrifuged on a self-forming Percoll gradient. ZGs at the bottom of the centrifuge tube were washed in isotonic buffer containing 50 mM Na-succinate for removal of mitochondrial contamination before use. To obtain ZGMs, ZGs were lysed in a hypotonic buffer containing a protease inhibitor cocktail, followed by centrifugation for 1 hr at 100,000 × g. In some experiments, alkaline washing with sodium carbonate was additionally performed to remove membrane-associated proteins following a modification of the protocol described by Fujiki et al. (1982). ZG lysate was diluted 1:50 in 250 mM sodium carbonate (pH 11.5) and incubated on ice for 30 min before centrifugation for 1 hr at 100,000 × g. Protein concentration was determined according to Bradford (1976).

Immunoblotting

HEK293 cells were transfected with control vectors or mCLCA plasmids as described previously and subsequently incubated in serum-containing medium. Twenty-four hr post-transfection, cells were harvested by trypsin digestion, washed twice in PBS at 4C, then washed in ice-cold homogenization buffer (12 mM HEPES + 300 mM mannitol, adjusted to pH 7.4, to which 100 μl/ml protease inhibitor cocktail was added immediately before use) and lysed on ice for 3 × 5 sec at 10 A using a Branson Sonicator 250 (Branson Ultrasonics; Danbury, CT). Immunoblotting of mCLCA1-6 proteins was performed according to standard protocols (Thévenod et al. 2003). Aliquots of lysate containing 25–50 μg of protein (or 80 μg of mouse pancreas homogenate, ZG, or ZGM) were heated for 5 min at 95C, subjected to 7.5% SDS-PAGE, and transferred onto polyvinylidene difluoride membranes. Blots were blocked with 3% non-fat dry milk and incubated overnight at 4C with 0.4 μg/ml–2 μg/ml of pAb849 against mCLCA1/2 or anti-FLAG M2 rabbit monoclonal antibody (1:10,000; Sigma-Aldrich Chemie, Taufkirchen, Germany). Following incubation with horseradish peroxidase (HRP)-conjugated donkey anti-rabbit or sheep anti-mouse secondary antibody (1:5000–10,000) (GE Healthcare Europe; Freiburg, Germany) for 1 hr at 4C, blots were developed using Western Lightning Plus chemiluminescence reagents (Perkin Elmer Life Sciences; Boston, MA) and signals were visualized on X-ray film. Specificity of the labeling was validated by incubating the blots with the primary antibody in the presence of 0.5 mM peptide antigen (ImuunoGlobe).

Immunoprecipitation

All steps were performed at 4C. Cell lysate (1 mg protein in 50 μl homogenization buffer) was mixed with 150 μl of radioimmunoprecipitation assay (RIPA) buffer [50 mM Tris-HCl (pH 8.0), 150 mM NaCl, 1% Nonidet P-40 (AppliChem; Darmstadt, Germany), 0.5% sodium deoxycholate, 0.1% SDS] and 10 μl protease inhibitor cocktail (Sigma-Aldrich Chemie). The solution was mixed for 45 min, and samples were centrifuged at high speed to remove particulate matter.

The supernatant was mixed with 1 μl of rabbit serum for preclearing and mixed again for 1 hr. Recombinant protein G sepharose 4B (8 μl of 25% suspension, washed in 50 mM Tris, pH 7.6, 150 mM NaCl) (Invitrogen) was added. After 30 min of incubation with agitation, the beads were removed by centrifugation and the extract was mixed with 10 μg anti-FLAG M2 monoclonal antibody or 10 μg pAb839; the mixture was gently vortexed and incubated for 1 hr. Protein G sepharose (25% suspension) was added (10 μl for FLAG-antibody and 50 μl for pAb849), vortexed, and incubated for a further 30 min. The beads were spun down for 1 min at top speed in a microfuge, the supernatant was discarded, and the beads were washed with 0.5 ml RIPA buffer. The beads were spun down as described above and washed once more with RIPA buffer. After centrifugation, the pellets were resuspended in loading buffer and heated for 5 min at 95C for SDS-PAGE.

Immunofluorescence Microscopy of mCLCA1-transfected HEK293 Cells

HEK293 cells were fixed with 4% paraformaldehyde, permeabilized for 15 min with 1% SDS, blocked for 1 hr with 1% BSA (all in PBS at room temperature), incubated overnight with pAb849 (0.4 μg/ml) at 4C, incubated for 1 hr at room temperature with donkey anti-rabbit antibody coupled to CyTM3 (Jackson ImmunoResearch Laboratories, Cambridgeshire, UK; diluted 1:600) followed by counterstaining with 0.8 μg/ml 2′-(4-ethoxyphenyl)-5-(4-methyl-1-piperazinyl)-2,5′-bi-1H-benzimidazole, 3HCl (H-33342) (Calbiochem; San Diego, CA) for 5 min. After three more 5-min washes in PBS, the cells were rinsed in dH_2O, and coverslips were mounted on glass slides with DAKO fluorescence mounting medium (DAKO; Hamburg, Germany). The cells were viewed using filters for Cy3 (red) and 4′,6-diamidino-2-phenylindole (blue) with excitation/emission wavelengths of 545/610 and 360/460 nm, respectively, using a mercury short-arc photo-optic lamp (HBO 103 W/2; OSRAM, Augsburg, Germany) as light source, which was connected to a Zeiss Axiovert 200M microscope (Carl Zeiss; Jena, Germany) equipped with a Fluar 40, 1.3 oil immersion objective. Images were captured using a digital CoolSNAP ES CCD camera (Roper Scientific; Tuscon, AZ) and acquired, processed, and analyzed with MetaMorph software (Universal Imaging; Downingtown, PA) (Abouhamed et al. 2007).

Immunohistochemistry

Fresh murine tissue samples were fixed in 4% neutral-buffered formaldehyde and routinely embedded in paraffin. The following organs and tissues were processed: kidneys, parotid, submandibular, and sublingual salivary gland, stomach, pancreas, and small intestine. The paraffin-embedded tissues were serially cut at 3 μm. Tissue sections were mounted on Superfrost Plus adhesive glass slides (Menzel-Gläser; Braunschweig, Germany). For immunohistochemical staining of paraffin-embedded tissue sections, the biotin-streptavidin–amplified method was applied (Leverkoehne and Gruber 2002). After dewaxing of the mounted tissue sections in xylene and rehydration in isopropanol and graded ethanol, antigen retrieval was performed by 15 min microwave heating (800 W). The sections were washed in PBS containing 0.01 M PBS and 0.05% Triton X-100 and afterwards blocked for 30 min in PBS containing 20% heat-inactivated normal goat serum. After repeated washes, the sections were incubated with the primary antibodies α-p3a1 (against aa 83–97 of mCLCA3; dilution 1:8000) (Leverkoehne and Gruber 2002), α-H^+/K^+-ATPase (Dianova, Hamburg, Germany, dilution 1:2000; a kind gift of Dr. Richard Warth, Department of Physiology, University of Regensburg, Germany) and pAb849 (dilutions ranging from 4 μg/ml to 20 μg/ml) in PBS/Tween 20 containing 1% BSA for 1 hr at room temperature. Sections were washed in PBS and incubated at room temperature for 1 hr with the polyclonal goat anti-rabbit immunoglobulins/alkaline phosphatase fast red TR (DAKO D0487) or biotinylated secondary goat anti-rabbit antibodies/HRP–coupled streptavidin, followed by repeated washes in PBS. Color was developed using either newfuchsin or diaminobenzidine as chromogens diluted in PBS, followed by repeated washes in PBS and rinsing in tap water. The slides were counterstained with hematoxylin, dehydrated through ascending graded ethanol, cleared in xylene, and coverslipped. Staining pattern and labeling intensity revealed no differences between paraffin and cryosections.

Confocal Laser-scanning Immunofluorescence Microscopy

For confocal laser scanning microscopy, paraffin-embedded tissue sections were processed as described previously, with minor modifications. The prepared tissue sections were incubated with secondary fluorochrome (FITC)-labeled goat anti-rabbit antibody (1:80) for 1 hr at room temperature. The nuclei were counterstained with TO-PRO-3 (Invitrogen) in a 1:1000 dilution for 5 min at room temperature and washed afterward. Finally, sections were mounted with ProLong Antifade reagent (Invitrogen). Fluorescent microscopy was performed using a confocal laser scanning microscope (TCS SP5; Leica Mikrosysteme Vertrieb, Wetzlar, Germany) for high-resolution microscopy. In control experiments, sections were incubated with the primary antibody in the presence of 1 mM peptide antigen. For double immunofluorescence, slides were incubated with goat anti-rabbit and donkey anti-mouse IgG coupled to

FITC (1:80) and Cy3 (1:600), respectively (Jackson Immunoresearch; Suffolk, UK). Sections were viewed with a Zeiss Axioplan2 with ApoTome module fluorescence microscope.

Laser-capture Microdissection and RNA Isolation

Adult female mice were sacrificed by cervical dislocation, and mouse parotid and submandibular gland tissue was quickly excised and immediately frozen in liquid N_2. Unfixed frozen tissue was subsequently cut in 10-μm cryosections and stained using standard histological techniques, such as hematoxylin and eosin staining. Parotid acinar and duct cells were selectively microdissected from the tissue sections using an ArcturusXT laser-capture microdissection microscope (AlphaMetrix Biotech; Roedermark, Germany). The microdissection approach ensures that biological molecules such as RNA and DNA remain unchanged during the microdissection process. Three animals were used for this study, and at least 10 sections from the submandibular gland and the parotid gland of each animal were necessary. For dissection of acinar and duct cells, 6000 and 3000 shots using a 15 μm infrared laser beam were used, respectively. All samples were prepared in duplicate. Dissected cells were extracted and processed for RNA extraction using the PicoPure RNA Isolation Kit (Arcturus) following the manufacturer's instructions. Total RNA has been isolated from dissected parotid acinar and duct cells using the Qiagen RNeasy kit (Hilden, Germany) and following the manufacturer's instructions. RNA integrity was evaluated using the 28S to 18S rRNA ratio on an RNA gel. Total RNA (0.5 μg)was reverse transcribed from an oligo(dT) primer using a Qiagen Omniscript kit.

RT-PCR of mCLCA1

The primers used for quantitative RT-PCR (qRT-PCR) were: forward primer, 5′-GTGGACCAGCCTTTCTACATGTCTAG-3′; reverse primer, 5′-TGTGACACAGTTGCCTCTCTCA-3′. They yielded a probe corresponding to nucleotides 525–638 of mCLCA1, GenBank accession no. NM 009899.3. Primers and probes were validated by analysis of a standard curve in a template dissociation curve. RT-PCR was performed according to the manufacturer's instructions (Applied Biosystems; Foster City, CA), as described elsewhere (Rickmann et al. 2007). Cycle conditions: denaturation at 95C for 10 min, and 40 cycles of PCR amplification at 95C for 15 sec and 61C for 30 sec, and elongation at 72C for 40 sec. All PCRs were performed in triplicate on an ABI PRISM 7500 Sequence Detection System (Applied Biosystems; Darmstadt, Germany). The mean ± SD of the cycle threshold (Ct) values for the *mCLCA1* gene and glyceraldehyde-3-phosphate dehydrogenase *(GAPDH)* were determined and analyzed for statistical significance using Student's unpaired *t*-test. Differences were considered statistically significant at $^*p<0.05$. For documentation of the data, relative mRNA levels were calculated using the comparative Ct method ($2^{-\Delta\Delta Ct}$), where the ΔΔCt value was calculated as follows: First, expression levels of the *mCLCA1* gene were normalized to a *GAPDH* signal {$\Delta Ct = Ct_{mCLCA1} - Ct_{GAPDH}$, $\Delta s = [s\ (mCLCA1)^2 + s\ (GAPDH)^2]^{0.5}$}. The value for ΔΔCt was then determined by: $\Delta\Delta Ct = \Delta Ct_{(parotid)} - \Delta Ct_{(submandibular)}$ or $\Delta\Delta Ct = \Delta Ct_{(parotid\ ducts)} - \Delta Ct_{(parotid\ acinar)}$, where the $\Delta Ct_{(submandibular)}$ and $\Delta Ct_{parotid\ acinar}$ was introduced as constant, respectively.

Preembedding Immunoperoxidase Electron Microscopy

Immunoperoxidase electron microscopy on fixed tissue sections was performed as described previously (Rickmann et al. 2007). Frozen sections (40-μm) from fixed mouse pancreas were cut and treated as described above for HRP immunohistochemistry. Subsequently, sections were osmicated in 1% OsO_4 and flat-embedded in epoxy medium. Selected sections were polymerized to the flat surface of an epoxy block, detached from the slide, and resectioned at 2-μm thickness. Optimally stained semithin sections were selected for a second resectioning process into ultrathin sections, which were stained with uranyl acetate and lead citrate before electron microscopic observation with a Zeiss EM 10 electron microscope.

Preembedding Immunogold Electron Microscopy

Electron microscopy on isolated rat pancreatic ZGs was performed as described previously (Thévenod et al. 2003), with minor modifications. ZGs were fixed in 2.5% glutaraldehyde in PBS for 1 hr and adsorbed onto poly-L-lysine–coated glass slides. Granules were washed with PBS for 10 min, treated sequentially with PBS containing 0.5% BSA, 0.5% gelatin, and 0.5% Tween 20 for 15 min; with PBS containing 0.05% BSA, 0.05% gelatin, and 0.05% Tween two times for 10 min; and then incubated with pAb849 (50 μg/ml) overnight at 4C. Samples were incubated with goat anti-rabbit IgG coupled to 10-nm gold particles (dilution 1:10) for 1 hr at room temperature, fixed with 1% glutaraldehyde in PBS for 30 min, and washed with water for 45 min. The gold particles were enlarged for 10 min using the silver enhancement kit from Aurion (Wageningen, The Netherlands). Samples were postfixed with 1% OsO_4 in 0.1 M sodium cacodylate for 10 min, treated with aqueous 2% uranyl acetate, dehydrated in a graded series of ethanol and propylene oxide, and embedded in Durcupan resin. Thin sections were counterstained with 2% uranyl acetate and lead citrate and viewed in a Zeiss EM 10

electron microscope. In controls, primary antibody was omitted.

Results

Antibody Characterization

mCLCA1 (accession no. gi:32964827) and mCLCA2 (accession no. gi:13447394) have 95% amino acid identity and therefore cannot be distinguished at the protein level by immunological approaches. Hence, we generated rabbit polyclonal antibodies against three different mCLCA1 peptides and screened the antisera by immunoblotting using crude membranes of mock-transfected or HEK293 cells transfected with FLAG-tagged mCLCA1. Based on an immunoreactive band of the expected molecular mass of ~125 kDa, pAb849 directed against a peptide (aa 424–443 of mCLCA1) that is common to mCLCA1/2 and had no significant amino acid similarity (≤80% identity) with the respective isoforms, mCLCA3-6 was selected for affinity immunopurification. Antibody validation was performed according to recently suggested guidelines (Bordeaux et al. 2010).

As shown in Figure 1A, in HEK293 cells transiently transfected with non–FLAG-tagged mCLCA1, the pAb849 (0.4 μg/ml) detected two specific protein bands, at ~125 kDa and 90 kDa (Figure 1A, Lane 4); many CLCA proteins, including mCLCA1, are synthesized as ~125-kDa precursor transmembrane glycoproteins that are rapidly cleaved into NH_2-terminal 90-kDa and COOH-terminal 35-kDa subunits (Pauli et al. 2000; Loewen and Forsyth 2005). The COOH-terminal 35-kDa fragment was not detected by pAb849 because of the more NH_2-terminal localization of the pAb949 peptide epitope. In contrast, in vector-transfected HEK293 cells, no specific signal was detected (Figure 1A, Lanes 1, 3, and 5), whereas a non-specific band at ~50 kDa was detected in all lanes, independently of the plasmid transfected. Lane 2 of Figure 1A shows that immunopurified pAb849 detected a single specific band of ~130 kDa in HEK293 cells transfected with FLAG-tagged mCLCA1. The

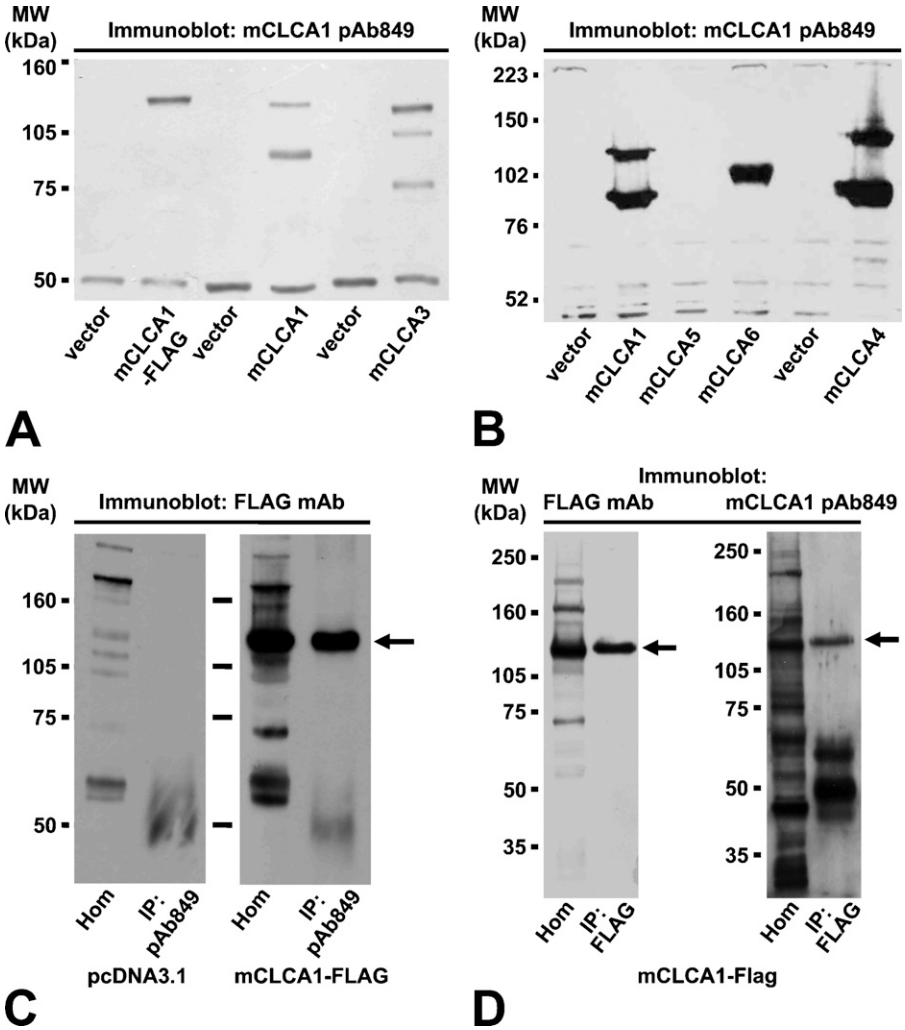

Figure 1 Generation and characterization of rabbit polyclonal antibody against mCLCA1/2. (**A,B**) HEK293 cells were transiently transfected with the respective plasmids or mock-transfected with the respective empty vector. Full-length mCLCA1 (~125 kDa) and its N-terminal cleavage product (~90 kDa) are detected by the pAb849 polyclonal antibody (0.4 μg/ml). The antibody also detected mCLCA3, mCLCA4, and mCLCA6, but not mCLCA5. (**C**) pAb849 was able to immunoprecipitate FLAG-tagged mCLCA1 expressed in HEK293 cells, which was detected by immunoblotting with FLAG antibody (1:10,000). Immunoreactive bands at ~125 kDa could be detected in mCLCA1-FLAG–transfected HEK293 cells, but not in mock-transfected HEK293 cells. (**D**) Anti-FLAG antibody was able to immunoprecipitate FLAG, as well as mCLCA1 expressed in mCLCA1-FLAG–transfected HEK293 cells, as detected by immunoblotting with anti-FLAG antibody and pAb849 (1 μg/ml), respectively. IP, immunoprecipitate; Hom, homogenate.

FLAG tag was introduced between aa 757 and aa 758, suggesting that this insert is so close to the putative cleavage site of mCLCA1 that it must prevent post-translational cleavage. Preimmune serum did not detect any of these bands in mCLCA1-transfected HEK293 cells (data not shown).

Transfection of HEK293 cells with mCLCA3 yielded three immunospecific bands (Figure 1A, Lane 6). A band that was detected at ~120 kDa probably represents the glycosylated full-length translation product, whereas two additional bands at ~100 kDa and ~75 kDa may reflect the primary translation product and the NH_2-terminal cleavage product, respectively, as suggested by Mundhenk et al. (2006). Immunoreactive bands similar to those of mCLCA1 could also be observed with pAb849 in HEK293 cells transfected with mCLCA4 (Figure 1B, Lane 6). In HEK293 cells transfected with mCLCA6, pAb849 reacted with a single protein band of ~105 kDa (Figure 1B, Lane 4), as previously described by Bothe et al. (2008), who used specific antibodies against the putative NH_2- and COOH-terminal cleavage products of mCLCA6 and observed only one immunospecific band. In contrast, in HEK293 cells transfected with mCLCA5 (Figure 1B, Lane 3), the pAb849 antibody did not detect any specific protein band, indicating that it does not recognize mCLCA5. As a conclusion, we were astonished that despite 20–40% differences in the amino acid sequence of the mCLCA1 epitope from the respective sequences of mCLCA3, mCLCA4, and mCLCA6 (Figure 2A), the antibody crossreacted with these isoforms. From these results, we also speculated that pAb849 might bind to the COOH-terminal amino acids of the peptide sequence (see Figure 2A).

The antibody pAb849 was also able to immunoprecipitate FLAG-tagged mCLCA1. As shown in Figure 1C, pAb849 immunoprecipitated a protein of ~125 kDa from HEK293 cells transfected with FLAG-tagged

A

Name	Sequence	Length	aa	Score
mCLCA1/2	CFEAVSRSGAIIHTIALGPS	20	424-443	-
mCLCA3	CFDLVKQSGAIIHTVALGPA	20	422-441	70
mCLCA4	CFQEVKHSGAIIHTIALGPS	20	427-446	80
mCLCA5	CLLTSMNSGSTIHSMALGSS	20	429-448	45
mCLCA6	CIDEVKDSGSIVHFIALGPS	20	424-443	60
	*: **: :* :***.:			

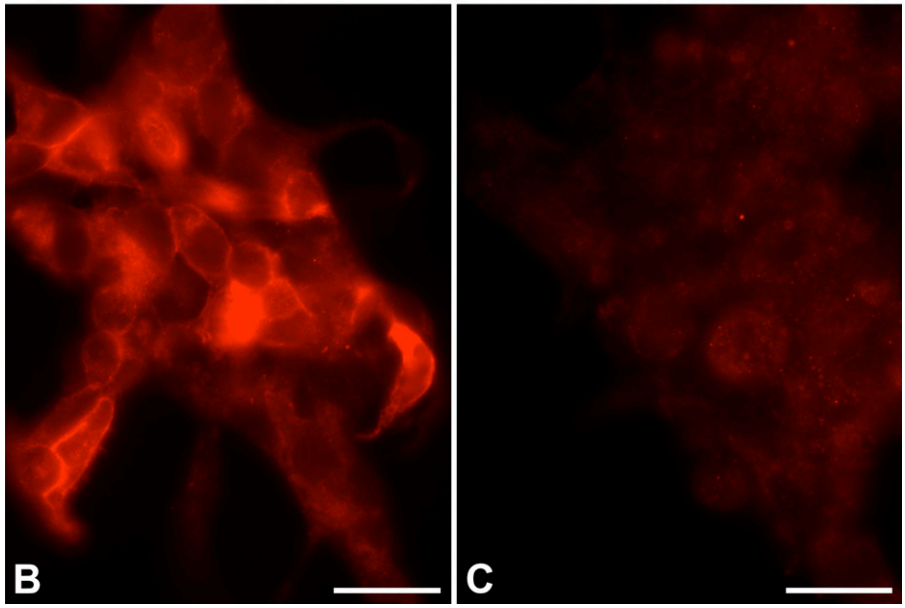

Figure 2 (**A**) Alignment of the peptide epitope sequence (aa 424–443 of mCLCA1) against which pAb849 rabbit polyclonal antiserum is directed, with the respective sequences of the known isoforms mCLCA3–mCLCA6. The amino acid sequence identity for mCLCA1:mCLCA3 was 70%; mCLCA1:mCLCA4, 80%; mCLCA1:mCLCA5, 45%; and mCLCA1:mCLCA6, 60%, as determined by ClustalW software (CLUSTAL 2.0.11). Key: red, small [small + hydrophobic (including aromatic −Y)]; blue, acidic; magenta, basic − H; green, hydroxyl + sulfhydryl + amine + G. Consensus symbols: *, identical; :, conserved substitutions; ., semi-conserved substitution. Subcellular localization of mCLCA1/2-Flag in HEK293 cells by immunofluorescence. HEK293 cells were transfected with pcDNA3.1 containing mCLCA1-Flag (**B**) or mock-transfected with pcDNA3.1. (**C**) mCLCA1-Flag was expressed in intracellular vesicular structures and in the periphery of HEK293 cells, suggesting plasma membrane localization (concentration of pAb849 0.4 μg/ml). Bar = 25 μm.

Table 1 Distribution of mCLCA isoforms in the gastrointestinal tract and kidney

	mCLCA isoform				
Tissue	1/2	3	4	5	6
Salivary glands	Acini (mRNA)[a] Ducts (protein)[b]	− (protein)[c]	− (mRNA)[d]	− (mRNA)[e]	− (protein)[f]
Pancreas	Acini (mRNA)[a] Acini (protein)[b]	− (protein)[c]	− (mRNA)[d]	+ (mRNA)[e]	− (protein)[f]
Stomach	Surface mucus cells + parietal cells (protein)[b]	Surface mucus cells (protein)[c]	− (mRNA)[d]	+ (mRNA)[e,g]	− (protein)[f]
Small intestine (jejunum)	Crypts (mRNA)[a] Crypts + goblet cells (protein)[b]	Goblet cells (protein)[c]	Villi + smooth muscles (mRNA)[d]	+ (mRNA)[e,g]	+ (mRNA)[e,g] Villi (small intestine) and Villi + crypts (large intestine) (protein)[f]
Kidney	Proximal + distal tubules (mRNA)[a] Distal tubules (protein)[b]	− (protein)[c]	− (mRNA)[d]	+ (mRNA)[e] − (mRNA)[g]	− (protein)[f]

[a]Gruber et al. 1998b.
[b]This study.
[c]Leverkoehne and Gruber 2002.
[d]Elble et al. 2002.
[e]Beckley et al. 2004.
[f]Bothe et al. 2008.
[g]Evans et al. 2004.
References from the literature and/or this study are specified by respective lower-case letters. Protein and/or mRNA expression is indicated in parentheses.

mCLCA1 that could be immunoblotted with anti-FLAG antibody (Figure 1C, arrow). This band was not detected in immunoprecipitated material from HEK293 cells transfected with pcDNA3.1 plasmid only (Figure 1C, Lane 2). In addition, as illustrated in Figure 1D, anti-FLAG antibody was able to immunoprecipitate a protein of ~125 kDa from HEK cells transfected with FLAG-tagged mCLCA1 that could be recognized by both anti-FLAG antibody (Figure 1D, Lane 2, arrow) and pAb849 (Figure 1D, Lane 4, arrow). Additional bands at ~50 kDa were not related to the immunospecificity of pAb849 for mCLCA1/2 (see also Figures 1A and 1B).

Immunofluorescence Staining of mCLCA1 Transfected Into HEK293 Cells Using pAb849

As illustrated in Figure 2B, mCLCA1 transfected into HEK293 cells showed intracellular punctate distribution, as visualized by immunofluorescence microscopy using pAb849 antibody (0.4 μg/ml) and CyTM3-coupled secondary antibodies (1:600), suggesting expression in vesicular structures. In addition, staining was found in the periphery of HEK293 cells, indicating plasma membrane localization. Only weak background staining was observed in mock-transfected cells (Figure 2C). We also determined the cellular distribution of FLAG-tagged mCLCA1 transfected into HEK293 cells, which does not show any posttranslational cleavage (see Figure 1A, Lane 2). The distribution was, however, similar to that of mCLCA1 (data not shown), suggesting that prevention of posttranslational cleavage does not affect cellular distribution and trafficking to the plasma membrane.

Immunolabeling of Exocrine Pancreas With pAb849

Because of the crossreactivity of pAb849 with mCLCA3, mCLCA4, and mCLCA6, we decided to limit our focus of interest exclusively to tissues that are known to express *mCLCA1/2* mRNA and do not express other mCLCA isoforms, or those in which the localization of this isoform (mCLCA3 and mCLCA6) has been already determined at the protein level (see Table 1).

Using in situ hybridization techniques, together with an oligonucleotide probe based on the *mCLCA1* sequence, Gruber et al. (1998b) previously demonstrated mRNA expression exclusively in the acini of the mouse pancreas. Subsequently, we have identified a CLCA

Figure 3 Cellular distribution of mCLCA1/2 in mouse pancreas. Localization of mCLCA1 protein in mouse pancreas was determined by immunoperoxidase (**A**), alkaline phosphatase (**B**), and immunofluorescence (**C,D**) light microscopy, on fixed paraffin sections. Immunoreactivity was detected in pancreatic acinar cells (A), exclusively expressed in zymogen granules (arrows). In contrast, in duct cells (D), labeling for mCLCA1 was absent. (**E**) mCLCA1/2 immunostaining was abolished after incubation of the sections with the pAb849 in the presence of 1 mM peptide antigen. (**F**) Immunoblot analysis of mouse pancreatic granule membranes with or without sodium carbonate extraction with the pAb849 antibody demonstrates immunolabeling of an ~130-kDa band (arrow) that was abolished in the presence of the peptide antigen. The blot is representative of three different experiments. Eighty μg protein was loaded onto each lane. (**G**) Preembedding immunoperoxidase electron microscopy on fixed pancreas sections. **(G/a)** Inset in **G** at higher magnification. L, lumen. mCLCA1/2 immunolabeling was observed in the zymogen granules (arrowheads) but not on the luminal plasma membrane (arrows). **(H,I)** Preembedding immunogold labeling by electron microscopy of isolated rat pancreatic zymogen granules in the presence (**H**) or absence (**I**) of pAb849 polyclonal antibody. Silver enhancement of gold particles.

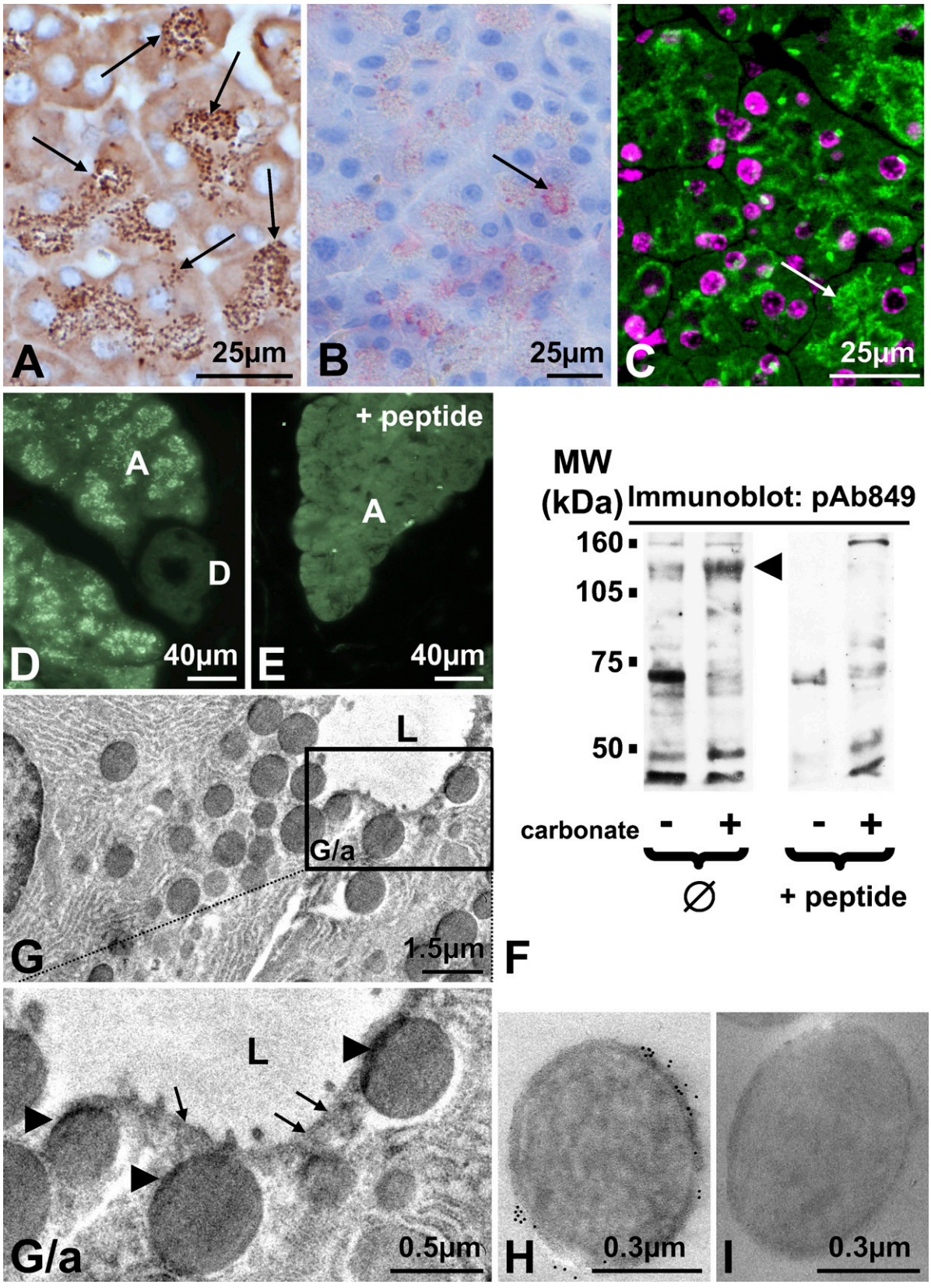

protein in rat ZGM with an antiserum against bovine CLCA1 that could be part of a Ca^{2+}-activated HCO_3^- conductance of rat ZGs (Thévenod et al. 2003). In the present study, we performed immunolabeling of mouse pancreatic tissue using three different techniques. When an HRP-coupled avidin–biotin complex was used with biotinylated secondary antibodies, color development with diaminobenzidine (DAB) as chromogen was found in pancreatic acini and associated with apical granular structures (Figure 3A, arrows). No staining was observed at acinar plasma membranes. Then the results were compared with those obtained using a second labeling procedure: the same technique was applied using alkaline phosphatase as reacting enzyme label and newfuchsin as chromogen. As shown in Figure 3B (arrow), in acinar cells, immunolabeling of moderate to strong intensity was observed. Immunostaining was not diffusely distributed in the cytoplasm, but showed a granular distribution preferentially located at the area occupied by the ZGs. Again, no plasma membrane staining was observed. These observations were confirmed by confocal laser scanning immunofluorescence microscopy, in which mCLCA1/2–specific staining (green fluorescent FITC labeling) was found localized beneath the apex of acinar cells (Figure 3C, arrow). Moreover, as illustrated in Figure 3D, pancreatic duct cells showed no staining at all. Similarly, apical and basolateral plasma membranes were devoid of immunofluorescence labeling. After incubation of the sections with the pAb849 antibody in the presence of 1 mM peptide antigen (Figure 3E), mCLCA1/2 labeling in the pancreas was abolished, demonstrating that the observed immunolabeling is indeed specific for mCLCA1/2.

Immunoblotting of ZGMs With pAb849

To complement these observations, ZGMs were purified from mouse pancreas and immunoblotted with pAb849. To verify whether mCLCA1/2 are indeed transmembrane proteins, ZGMs were isolated after sodium carbonate wash, as described in Materials and Methods. Regardless of the isolation protocol used, a protein band was detected at ~130 kDa in ZGMs (Figure 3F, arrow) that was more prominent after sodium carbonate wash, suggesting enrichment of full-length mCLCA1/2 in this fraction. An ~75-kDa immunoreactive band was also present. Incubation of the blots with the pAb849 antibody that had been preincubated with 0.5 mM of the respective peptide antigen abolished the ~130-kDa band, but not the lower-molecular-mass band, demonstrating that the ~130-kDa band is specific for mCLCA1/2.

Electron Microscopy of ZGMs Labeled With pAb849

To ensure that labeling observed in acinar cells indeed represented immunoreactivity of ZGMs, mCLCA1/2 protein expression in pancreatic ZGs was further determined at the ultrastructural level, by preembedding immunoperoxidase electron microscopy on fixed pancreatic tissue sections (Figure 3G), as well as by immunogold labeling on purified mouse pancreatic ZGs (Figures 3H and 3I). As illustrated in Figure 3G, lateral plasma membrane of acinar cells was devoid of mCLCA1/2 immunoreactivity. In contrast, ZGs exhibited mCLCA1/2 immunoreactivity that was restricted to the surface of the granules, thus representing labeling of the ZGMs. Higher magnification shown in the insert in Figure 3G, also highlights the absence of mCLCA1/2 immunolabeling of the luminal acinar membrane (arrows), whereas ZGMs were strongly labeled (arrowheads). Finally, immunogold labeling of isolated ZGs (Figure 3H) also confirmed that mCLCA1/2 immunoreactivity was exclusively located at the surface of the granules. In the absence of the primary antibody, no labeling could be detected (Figure 3I).

Expression of mCLCA1 mRNA in Mouse Salivary Glands

A previous study demonstrated *mCLCA1* mRNA expression in the acini of mouse salivary glands by in situ hybridization (Gruber et al. 1998b). Figure 4 shows relative expression levels of *mCLCA1* in mouse parotid gland and submandibular gland primary tissue (Figure 4A), as well as in laser-microdissected parotid acinar and duct cells (Figure 4B) by qRT-PCR analysis using *mCLCA1*-specific primers. *mCLCA1* expression was significantly higher in mouse parotid gland, compared with submandibular gland ($p=0.015$; $n=3$). Within the parotid gland, however, acinar and duct cells exhibited comparable levels of *mCLCA1* mRNA (Figure 4B; $p=0.94$; $n=3$).

Immunostaining of Salivary Glands With pAb849

Localization of mCLCA1/2 protein was investigated on fixed paraffin sections of mouse parotid, submandibular, and sublingual glands using the pAb849 antibody and the biotin-streptavidin–amplified method with either alkaline phosphatase or HRP as reacting enzyme. Individual glands revealed a distinct mCLCA1/2 labeling pattern. As illustrated in Figure 4C, acinar cells of mouse parotid gland revealed intracellular mCLCA1/2 labeling of moderate to strong intensity. In striated duct cells, immunoreactivity for mCLCA1/2 was observed at the apical membrane. In contrast, blood vessels were devoid of mCLCA1/2 immunostaining (Figure 4D). In the submandibular gland, mCLCA1/2 staining was absent in acinar cells (Figures 4E and 4F), but duct cells of the submandibular gland revealed a complex labeling pattern. Whereas mCLCA1/2 immunoreactivity was weak in the luminal membrane of striated ducts, granular duct cells (Figures 4E and 4F), i.e., the duct segment

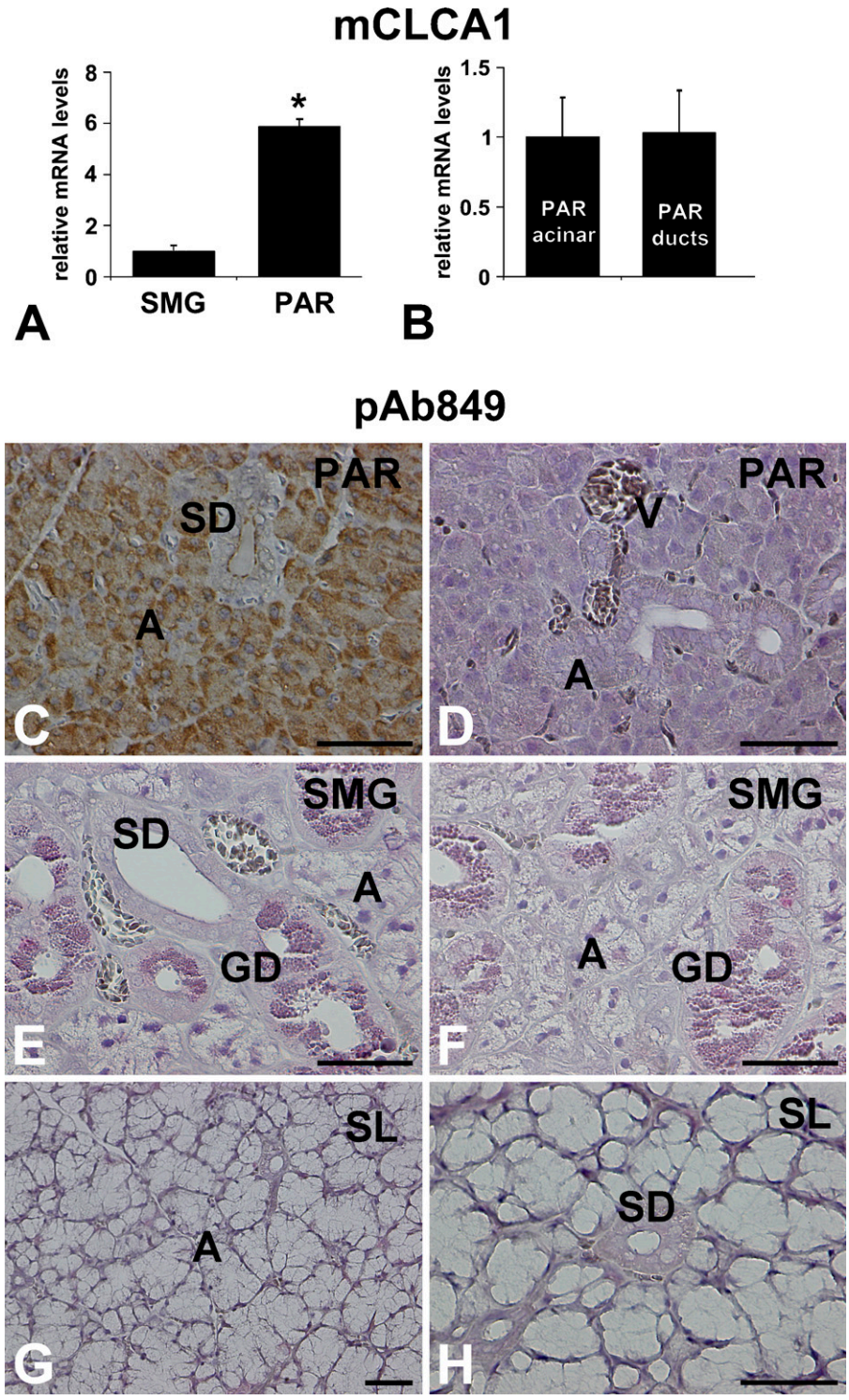

Figure 4 Expression of mCLCA1/2 in mouse salivary glands. (**A**) RT-PCR analysis for relative *mCLCA1/2* expression levels in mouse submandibular gland (SMG) and parotid gland (PAR). Expression of *mCLCA1* is shown as $2^{-\Delta\Delta Ct \pm s}$. Expression level of *mCLCA1* in mouse submandibular gland was set as reference. (**B**) mCLCA1/2 expression was found in acinar and duct cells of mouse parotid gland, the two compartments exhibiting comparable expression levels. (**C–H**) Fixed paraffin sections of mouse salivary glands were immunolabeled with the pAb849 antibody directed against mCLCA1/2 and developed using second antibodies coupled to alkaline phosphatase or peroxidase. In mouse PAR, mCLCA1/2 immunoreactivity was localized apically in striated (SD) duct cells and intracellularly in acinar cells (A). Granular duct cells (GD) of mouse SMG revealed strong mCLCA1/2 immunolabeling, whereas striated duct cells showed weak mCLCA1/2 immunoreactivity and acinar cells (A) were devoid of mCLCA1/2 expression. In sublingual gland (SL) tissue, protein expression of mCLCA1/2 was not detected. V, blood vessel. *$p<0.05$ statistical significance using Student's unpaired *t*-test. Bar = 50 μm.

of male rodent submandibular gland that lies between intercalated and striated ducts, exhibited strong mCLCA1/2 labeling. This staining pattern was neither diffusely distributed in the cytoplasm nor observed in the luminal membrane, but was clearly restricted to the granules. Finally, in the sublingual gland, both acinar (Figure 4G) and duct cells (Figure 4H) were devoid of mCLCA1/2 immunolabeling.

Immunostaining of Stomach, Small Intestine, and Kidney With pAb849

Cellular distribution of mCLCA1/2 in murine intestinal tissues is shown in Figures 5A–5H. When fixed paraffin sections of these tissues were investigated with pAb849 and the biotin-streptavidin–amplified method with alkaline phosphatase as reacting enzyme, stomach showed immunostaining of epithelial cells lining the lumen (Figure 5A, arrows). These cells represent mucous cells, as ensured by periodic acid-Schiff histological staining (data not shown). In addition, gastric parietal cells (Figure 5B, arrows) were also immunoreactive for mCLCA1/2. To verify the nature of labeled cells, double immunofluorescence with H^+/K^+-ATPase (Figure 5C), a marker for parietal cells, and pAb849 (Figure 5D) was performed. Overlay revealed colocalization of the proteins in parietal cells (Figure 5E, arrows). In jejunum, mCLCA1/2 staining was observed in goblet cells and apical areas of crypt cells (Figure 5F, arrows). Similar results were obtained using HRP as reacting enzyme (Figure 5G, green and yellow arrows). Staining of intramural plexus (Figure 5G, red arrows) may also indicate specific mCLCA1/2 expression. Because mCLCA3 protein is known to be expressed exclusively in mucin granules of intestinal mucous and goblet cells, including stomach and small intestine, where its cleavage products are known to be secreted soluble proteins (Leverkoehne and Gruber 2002; Mundhenk et al. 2006), and based on the observation that pAb849 crossreacts with mCLCA3, it was necessary to differentiate the nature of the labeling obtained. When sections were immunostained with α-p3a1 against aa 83–97 of mCLCA3 (Leverkoehne and Gruber 2002), expression of mCLCA3 was found exclusively in mucous and goblet cells (green arrows in Figure 5H and data not shown), suggesting that apical staining of crypt and parietal cells is specific for mCLCA1/2.

Previous studies have demonstrated mCLCA1/2 mRNA expression in proximal tubules and, to a much lesser extent, in Henle loop and distal tubules by in situ hybridization (Gruber et al. 1998b), whereas other CLCA isoforms were not detected (see Table 1). Using pAb849 on fixed mouse kidney sections, strong immunoreactivity could be found in distal tubules (Figure 5I). In renal proximal tubules, mCLCA1/2 immunoreactivity was considerably weaker, compared with that of distal tubules, but nevertheless detectable (Figure 5I). In addition, mCLCA1/2 labeling was observed in renal collecting duct cells (data not shown).

Discussion

The aim of this study was to determine the cellular distribution and subcellular localization of mouse CLCA1 and CLCA2 (mCLCA1/2) in epithelia, as a first step toward determining their role in these tissues. To that end, we have generated and characterized rabbit polyclonal antibodies against mCLCA1/2 following state of the art experimental approaches (Bordeaux et al. 2010). mCLCA1 (accession no. gi32964827) and mCLCA2 (accession no. gi13447394) have 95% amino acid identity and therefore cannot be distinguished at the protein level. In mCLCA1-transfected HEK293 cells, the generated pAb849 antibody recognized specific bands at ~125 kDa and ~90 kDa, corresponding to the molecular mass of the mCLCA1 precursor glycoprotein and its NH_2-terminal cleavage product, respectively. Notably, FLAG-tagged mCLCA1 prevented cleavage of the protein, confirming and extending previous observations, which showed that epitope insertion experiments result in misfolding of the protein and subsequent absence of cleavage (Gruber et al. 1998a). The generated pAb849 antibody recognized mCLCA3, mCLCA4, and mCLCA6 as well, but not mCLCA5, as assessed by immunoblotting (Figures 1A and 1B). Because pAb849 was generated against an oligopeptide sequence of mCLCA1/2 that shares 70%, 80%, 45%, and 60% homology with the respective sequences of mCLCA3, mCLCA4, mCLCA5, and mCLCA6 (Figure 2A), it is conceivable to assume that the pAb849 might bind to the COOH-terminal amino acids of the epitope sequence.

We have used this antibody as a tool to determine cellular distribution of mCLCA1/2 in mouse salivary glands, pancreas, stomach, small intestine, and kidney, epithelia significantly involved in transepithelial fluid transport and protein secretion. Among the organs examined, salivary glands and pancreas express only mCLCA1/2 and no other mCLCA isoform (Elble et al. 2002; Leverkoehne and Gruber 2002; Beckley et al. 2004; Bothe et al. 2008). Through a combination of several experimental approaches, including immunoblotting, immunohistochemistry, and immunoelectron microscopy, mCLCA1/2 protein expression in mouse

Figure 5 Cellular distribution of mCLCA1/2 in mouse stomach (**A–E**), small intestine (**F–H**), and kidney (**I**). Immunohistochemistry on fixed mouse tissue sections using the pAb849 antibody. Surface mucous cells (**A,** arrows) and gastric parietal cells (**B,** arrows) showed mCLCA1/2 immunoreactivity. (**C–E**) Double labeling with H^+/K^+-ATPase (**C**) and pAb849 (**D**) revealed colocalization of the proteins in gastric parietal cells (**E,** arrows). (**F**) Labeling in goblet cells and in the apical pole of crypt cells of small intestine was also detectable. (**G**) Green arrows point to staining in goblet cells, yellow arrows indicate luminal staining in epithelial crypt cells, and red arrows point to intramural plexus. (**H**) Using an antibody specific against mCLCA3 (pAb α-p3A1), goblet cells of small intestine (green arrows) were labeled. (**I**) Using the pAb849 antibody on fixed mouse kidney sections, strong mCLCA1/2 immunostaining was observed in distal tubules (DT). Proximal tubules (PT) revealed weak mCLCA1/2 labeling at their luminal membranes. Bars: **A,B,F–I** = 100 μm; **C–E** = 50 μm.

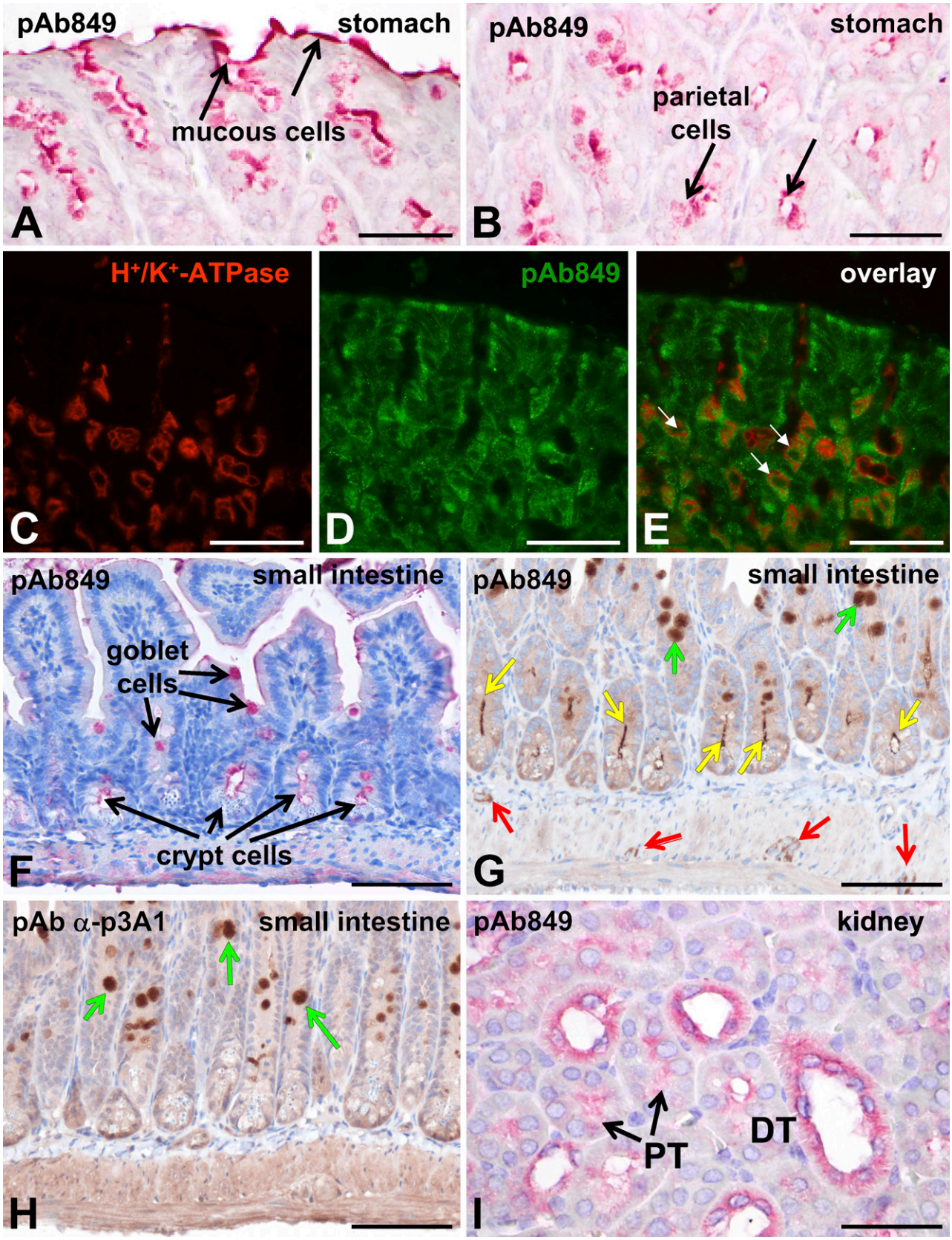

The Journal of Histochemistry & Cytochemistry

pancreas was found to be restricted to ZGMs (Figure 3). Notably, expression of mCLCA1/2 in ZGMs that had been isolated after alkaline washing with carbonate was increased, compared with that observed in ZGMs isolated following standard protocols, thus highlighting that mCLCA1/2 in ZGs are transmembrane proteins (Figure 3F). These data extend previous results that have shown *mCLCA1/2* gene expression in mouse pancreatic acinar cells (Gruber et al. 1998b), confirming our previous study showing expression of an ~120-kDa protein in rat ZGMs using a polyclonal antibody against the bovine trachea CLCA1 subunit (Thévenod et al. 2003). In that study, we also suggested that a CLCA-related protein could contribute to a Ca^{2+}-activated HCO_3^- conductance in rat pancreatic ZGMs and to hormone-stimulated secretion (Thévenod et al. 2003). The notion that ion conductances in pancreatic ZGs regulate exocytosis is not novel (for review, see Thévenod 2002). The recently cloned CaCC TMEM16A exhibits cellular distribution in pancreas identical to that shown by mCLCA1/2 (Yang et al. 2008). These data are not contradictory to the results of the present study, but, rather, might implicate redundancy of anion conductances in ZGMs, or mCLCA1/2 might regulate the anion channel. It remains to be determined whether mCLCA1/2 and TMEM16A physically interact and whether TMEM16A plays a role in exocytosis.

The distribution pattern of mCLCA1/2 in mouse salivary glands proved to be gland specific (Figure 4). The results of the qRT-PCR using specific *mCLCA1* primers showed mRNA expression for *mCLCA1* in mouse parotid gland, observations in accordance with previous reports by in situ hybridization using a probe that recognized *mCLCA1/2* (Gruber et al. 1998b) and qRT-PCR for *mCLCA1* and *mCLCA2* expression in murine parotid gland (Leverkoehne et al. 2002). Expression of mCLCA2 in the mouse parotid gland has not been determined in the present study, but it has been shown that *mCLCA1* and *mCLCA2* expressions in mouse parotid gland are of similar magnitude (Leverkoehne et al. 2002). The results of the present study extend previous observations and demonstrate for the first time *mCLCA1* expression in mouse submandibular gland, although the expression level is considerably lower than that in parotid gland. In addition, we provide first evidence that *mCLCA1/2* are additionally expressed in parotid ducts. Because other mCLCA isoforms are not expressed in salivary glands, the data observed here are specific for mCLCA1/2. Using the pAb849 antibody, mCLCA1/2 were found localized in the cytoplasm of parotid acinar cells, and at the luminal membrane of duct cells. According to the established model for electrolyte transport in salivary glands, acinar cells produce a NaCl-rich primary fluid, which becomes modified in the duct system by reabsorption of Na^+ and Cl^- (Melvin et al. 2005). To fulfill these functions, several classes of channels are thought to be localized in the luminal membranes of salivary acinar and duct cells, including CaCCs (Zeng et al. 1997), whose molecular identities are still not known (Melvin et al. 2005). The rat homolog rCLCA1 exhibits 83% amino acid identity with mCLCA1 and mCLCA2 and is absent in acinar cells but localized in the apical membrane of rat parotid striated and rat submandibular granular and striated duct cells (Yamazaki et al. 2005; Ishibashi et al. 2006). In vivo, *rCLCA* siRNA in submandibular ducts significantly increased Cl^- concentration in the final saliva during stimulation with pilocarpine, implicating the involvement of rCLCA in ductal Cl^- reabsorption (Ishibashi et al. 2006). In the present study, we also showed weak but nevertheless detectable luminal mCLCA1/2 immunolabeling in striated ducts of the submandibular gland. Moreover, mCLCA1/2 staining was also present in the mouse granular ducts of the submandibular gland, a sexually dimorphic duct segment in rodents. Granular duct cells are characterized by an abundance of secretory granules that contain biologically active polypeptides, including growth factors and proteolytic enzymes, and undergo multihormonal regulation. Although the physiological significance of this distribution pattern is not clear, mCLCA1/2 might be involved in secretagogue-induced enzyme secretion in this duct segment. The differences in rCLCA1 and mCLCA1/2 distribution in salivary acinar cells could be explained by species-specific CLCA1 localization, resembling distribution of other channels and transporters. In contrast, the predominant mucous sublingual gland was devoid of mCLCA1/2 expression, similar to previously observed mCLCA3 expression (Leverkoehne and Gruber 2002). To elucidate whether mCLCA1 might need auxiliary proteins as cofactors to exert its function, additional studies will be needed.

Whereas the labeling obtained with the pAb849 in mouse salivary glands and pancreas could be easily identified as mCLCA1/2, the staining pattern in other epithelia of the gastrointestinal tract proved to be more challenging. In murine stomach, immunoreactivity in surface mucous and in parietal cells was detectable (Figures 5A–5E), in agreement with previous observations by in situ hybridization (Gruber et al. 1998b). In the small intestine, goblet cells and apical cell sides of crypt cells were stained (Figures 5F and 5G). However, surface mucous cells of the stomach and intestinal goblet cells express mCLCA3 as well, and *mCLCA5* mRNA has also been reported in the stomach and small intestine (Leverkoehne and Gruber 2002; Beckley et al. 2004; Evans et al. 2004). Taking into consideration that the pAb849 does not recognize mCLCA5, together with the observation that a specific antibody against mCLCA3 selectively immunolabeled surface mucous and goblet cells in small intestine (Figure 5H),

it can be concluded that labeling in parietal cells in the stomach and in the apical pole of crypt cells in small intestine is indeed mCLCA1/2 specific. In the kidney, mCLCA1/2 were found in the distal tubule cells and, to a lesser extent, localized to the apical membranes of proximal tubule cells, extending previous observations by qRT-PCR and in situ hybridization (Figure 5I).

Taking the results of the present study together, it becomes clear that the mCLCA1/2 distribution pattern is prominent in cell membranes in all epithelia examined, suggesting that mCLCA1/2 are integral membrane proteins. The presence of mCLCA1/2 in ZGMs underscores this observation. This seems to be different from mCLCA3, which is a secretory protein (Mundhenk et al. 2006), but similar to mCLCA6, which is expressed in apical membranes of villous enterocytes in the small intestine and in villi and crypts of the large intestine (Bothe et al. 2008). The reason for these differences of localization between mCLCA isoforms is not clear. One explanation could be the differences of the protein structure in mCLCA/2 and mCLCA3. In contrast to mCLCA3, mCLCA1/2 hydrophobicity plots reveal hydrophobic transmembrane regions near the C terminus of the protein, supporting the notion that this protein is membrane associated.

In conclusion, we have generated antibodies against mCLCA1/2 and determined cellular distribution in mouse gastrointestinal tract and kidney. The apical localization of mCLCA1/2 in salivary duct cells, renal tubules, parietal cells, and epithelial cells of the small intestinal crypts, together with its expression on the pancreatic zymogen granule membrane, argues against a secreted protein and favors a cell type–specific function of mCLCA1/2 contributing to protein secretion and transepithelial ion transport.

Acknowledgments

The study was supported by the Deutsche Forschungsgemeinschaft (grant RO 2495/1-3 to ER). The laboratory of F.T. is funded by grants from the Deutsche Forschungsgemeinschaft and a grant from the Deutsche Mukoviszidose e.V. (F04/04).

Literature Cited

Abouhamed M, Wolff NA, Lee WK, Smith CP, Thévenod F (2007) Knockdown of endosomal/lysosomal divalent metal transporter 1 by RNA interference prevents cadmium-metallothionein-1 cytotoxicity in renal proximal tubule cells. Am J Physiol Renal Physiol 293:F705–712

Agnel M, Vermat T, Culouscou JM (1999) Identification of three novel members of the calcium-dependent chloride channel (CaCC) family predominantly expressed in the digestive tract and trachea. FEBS Lett 455:295–301

Beckley JR, Pauli BU, Elble RC (2004) Re-expression of detachment-inducible chloride channel mCLCA5 suppresses growth of metastatic breast cancer cells. J Biol Chem 279:41634–41641

Bordeaux J, Welsh AW, Agarwal S, Killiam E, Baquero MT, Hanna JA, Anagnostou VK, et al. (2010) Antibody validation. Biotechniques 48:197–209

Bothe MK, Braun J, Mundhenk L, Gruber AD (2008) Murine mCLCA6 is an integral apical membrane protein of non-goblet cell enterocytes and co-localizes with the cystic fibrosis transmembrane conductance regulator. J Histochem Cytochem 56: 495–509

Bradford MM (1976) A rapid and sensitive method for the quantitation of microgram quantities of protein utilizing the principle of protein-dye binding. Anal Biochem 72:248–254

Caputo A, Caci E, Ferrera L, Pedemonte N, Barsanti C, Sondo E, Pfeffer U, et al. (2008) TMEM16A, a membrane protein associated with calcium-dependent chloride channel activity. Science 322:590–594

Elble RC, Ji G, Nehrke K, DeBiasio J, Kingsley PD, Kotlikoff MI, Pauli BU (2002) Molecular and functional characterization of a murine calcium-activated chloride channel expressed in smooth muscle. J Biol Chem 277:18586–18591

Evans SR, Thoreson WB, Beck CL (2004) Molecular and functional analyses of two new calcium-activated chloride channel family members from mouse eye and intestine. J Biol Chem 279: 41792–41800

Fujiki Y, Hubbard AL, Fowler S, Lazarow PB (1982) Isolation of intracellular membranes by means of sodium carbonate treatment: application to endoplasmic reticulum. J Cell Biol 93:97–102

Gandhi R, Elble RC, Gruber AD, Schreur KD, Ji HL, Fuller CM, Pauli BU (1998) Molecular and functional characterization of a calcium-sensitive chloride channel from mouse lung. J Biol Chem 273:32096–32101

Gibson A, Lewis AP, Affleck K, Aitken AJ, Meldrum E, Thompson N (2005) hCLCA1 and mCLCA3 are secreted non-integral membrane proteins and therefore are not ion channels. J Biol Chem 280:27205–27212

Greenwood IA, Miller LJ, Ohya S, Horowitz B (2002) The large conductance potassium channel beta-subunit can interact with and modulate the functional properties of a calcium-activated chloride channel, CLCA1. J Biol Chem 277:22119–22122

Gruber AD, Elble RC, Ji HL, Schreur KD, Fuller CM, Pauli BU (1998a) Genomic cloning, molecular characterization, and functional analysis of human CLCA1, the first human member of the family of Ca2+-activated Cl- channel proteins. Genomics 54:200–214

Gruber AD, Gandhi R, Pauli BU (1998b) The murine calcium-sensitive chloride channel (mCaCC) is widely expressed in secretory epithelia and in other select tissues. Histochem Cell Biol 110:43–49

Hartzell C, Putzier I, Arreola J (2005) Calcium-activated chloride channels. Annu Rev Physiol 67:719–758

Ishibashi K, Yamazaki J, Okamura K, Teng Y, Kitamura K, Abe K (2006) Roles of CLCA and CFTR in electrolyte re-absorption from rat saliva. J Dent Res 85:1101–1105

Lee WK, Torchalski B, Roussa E, Thévenod F (2008) Evidence for KCNQ1 K+ channel expression in rat zymogen granule membranes and involvement in cholecystokinin-induced pancreatic acinar secretion. Am J Physiol Cell Physiol 294:C879–892

Leverkoehne I, Gruber AD (2002) The murine mCLCA3 (alias gob-5) protein is located in the mucin granule membranes of intestinal, respiratory, and uterine goblet cells. J Histochem Cytochem 50: 829–838

Leverkoehne I, Horstmeier BA, von Samson-Himmelstjerna G, Scholte BJ, Gruber AD (2002) Real-time RT-PCR quantitation of mCLCA1 and mCLCA2 reveals differentially regulated expression in pre- and postnatal murine tissues. Histochem Cell Biol 118:11–17

Loewen ME, Forsyth GW (2005) Structure and function of CLCA proteins. Physiol Rev 85:1061–1092

Melvin JE (1999) Chloride channels and salivary gland function. Crit Rev Oral Biol Med 10:199–209

Melvin JE, Yule D, Shuttleworth T, Begenisich T (2005) Regulation of fluid and electrolyte secretion in salivary gland acinar cells. Annu Rev Physiol 67:445–469

Mundhenk L, Alfalah M, Elble RC, Pauli BU, Naim HY, Gruber AD (2006) Both cleavage products of the mCLCA3 protein are secreted soluble proteins. J Biol Chem 281:30072–30080

Patel AC, Brett TJ, Holtzman MJ (2009) The role of CLCA proteins in inflammatory airway disease. Annu Rev Physiol 71:425–449

Pauli BU, Abdel-Ghany M, Cheng HC, Gruber AD, Archibald HA, Elble RC (2000) Molecular characteristics and functional diversity of CLCA family members. Clin Exp Pharmacol Physiol 27:901–905

Rickmann M, Orlowski B, Heupel K, Roussa E (2007) Distinct expression and subcellular localization patterns of Na+/HCO3- cotransporter (SLC 4A4) variants NBCe1-A and NBCe1-B in mouse brain. Neuroscience 146:1220–1231

Schroeder BC, Cheng T, Jan YN, Jan LY (2008) Expression cloning of TMEM16A as a calcium-activated chloride channel subunit. Cell 134:1019–1029

Thévenod F (2002) Ion channels in secretory granules of the pancreas and their role in exocytosis and release of secretory proteins. Am J Physiol Cell Physiol 283:C651–672

Thévenod F, Roussa E, Benos DJ, Fuller CM (2003) Relationship between a HCO3-permeable conductance and a CLCA protein from rat pancreatic zymogen granules. Biochem Biophys Res Commun 300:546–554

Williams JA (2006) Regulation of pancreatic acinar cell function. Curr Opin Gastroenterol 22:498–504

Yamazaki J, Okamura K, Ishibashi K, Kitamura K (2005) Characterization of CLCA protein expressed in ductal cells of rat salivary glands. Biochim Biophys Acta 1715:132–144

Yang YD, Cho H, Koo JY, Tak MH, Cho Y, Shim WS, Park SP, et al. (2008) TMEM16A confers receptor-activated calcium-dependent chloride conductance. Nature 455:1210–1215

Zeng W, Lee MG, Muallem S (1997) Membrane-specific regulation of Cl- channels by purinergic receptors in rat submandibular gland acinar and duct cells. J Biol Chem 272:32956–32965

The Journal of Histochemistry & Cytochemistry